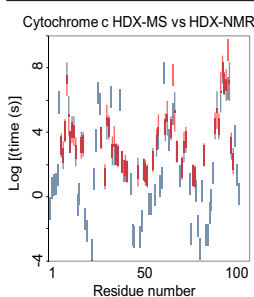


RESEARCH ARTICLE

Determination of Equine Cytochrome c Backbone Amide Hydrogen/Deuterium Exchange Rates by Mass Spectrometry Using a Wider Time Window and Isotope Envelope

Yoshitomo Hamuro

ExSAR Corporation, 11 Deer Park Drive, Suite 103, Monmouth Junction, NJ 08852, USA



Abstract. A new strategy to analyze amide hydrogen/deuterium exchange mass spectrometry (HDX-MS) data is proposed, utilizing a wider time window and isotope envelope analysis of each peptide. While most current scientific reports present HDX-MS data as a set of time-dependent deuteration levels of peptides, the ideal HDX-MS data presentation is a complete set of backbone amide hydrogen exchange rates. The ideal data set can provide single amide resolution, coverage of all exchange events, and the open/close ratio of each amide hydrogen in EX2 mechanism. Toward this goal, a typical HDX-MS protocol was modified in two aspects: measurement of a wider time window in HDX-MS experiments and deconvolution of isotope envelope of each peptide. Measurement of a wider time window enabled the observation of

deuterium incorporation of most backbone amide hydrogens. Analysis of the isotope envelope instead of centroid value provides the deuterium distribution instead of the sum of deuteration levels in each peptide. A one-step, global-fitting algorithm optimized exchange rate and deuterium retention during the analysis of each amide hydrogen by fitting the deuterated isotope envelopes at all time points of all peptides in a region. Application of this strategy to cytochrome *c* yielded 97 out of 100 amide hydrogen exchange rates. A set of exchange rates determined by this approach is more appropriate for a patent or regulatory filing of a biopharmaceutical than a set of peptide deuteration levels obtained by a typical protocol. A wider time window of this method also eliminates false negatives in protein-ligand binding site identification.

Keywords: Cytochrome *c*, Hydrogen/deuterium exchange, Isotope envelope, Mass spectrometry

Abbreviations: CID, Collision induced dissociation; ETD, Electron transfer dissociation; GuHCl, Guanidine hydrochloride; HDX, Hydrogen/deuterium exchange; LC, Liquid chromatography; MS, Mass spectrometry; MS/MS, Tandem mass spectrometry; TFA, Trifluoroacetic acid

Received: 19 September 2016/Revised: 2 November 2016/Accepted: 27 November 2016/Published Online: 20 January 2017

Introduction

Hydrogen/deuterium exchange coupled with proteolysis, liquid chromatography (LC), and mass spectrometry (HDX-MS), is becoming a standard method to characterize proteins. The technique can be used for protein characterization [1–4], protein–small molecule interactions [5–7], and protein–protein interactions [8–11]. A typical HDX reaction performed

in deuterated buffer at near neutral pH is followed by quenching of the reaction by the addition of a cold acidic buffer, digestion by protease(s) active at low pH, LC separation, and MS analysis.

The ideal HDX-MS data set presents the exchange rate of each backbone amide hydrogen for the entire sequence of an analyte protein. To acquire this type of data, two dimensions have to be considered: protein sequence resolution and exchange time window [12]. A conventional HDX-MS data set presents total deuterium incorporations in medium resolution (several amide hydrogens) for a relatively narrow time window (2–3 orders of magnitude). The medium resolution of the data makes it very difficult to pinpoint where interesting behavior(s) occurred in the segment. A narrow time window often fails to

Electronic supplementary material The online version of this article (doi:10.1007/s13361-016-1571-1) contains supplementary material, which is available to authorized users.

Correspondence to: Yoshitomo Hamuro; e-mail: yhamuro@yahoo.com

detect important exchange event(s) of very fast and very slow exchanging amide hydrogens.

Achieving single amide resolution in HDX-MS is an active research area. There are two fundamentally different approaches: sublocalization of deuterium by subtraction of the deuteration levels in two analogous peptic or ion fragments, and utilization of the isotope envelope shape [13] instead of the centroid value of a peptic fragment [14–17]. The sublocalization method can be further dissected into three subclasses: utilization of non-specificity of a single protease such as pepsin [12, 18, 19], development of new proteases [20–24], and fragmentation of a peptide in the gas phase [25–30].

Sublocalization method subtracts the deuteration levels of two analogous peptic or ion fragments. In this method, for example, the subtraction of the number of deuteriums in residues 1–9 from that in residues 1–10 can yield the deuteration level in residue 10. Good signal-to-noise ratio of both fragments is critical for this approach, due to the propagation of error upon subtraction.

Sublocalization utilizing only analogous pepsin fragments is possible and has been used since early days of HDX-MS analysis [18, 19]. This method takes advantage of relative weak sequence specificity of pepsin [31]. This method works well as long as HDX-MS system can generate and detect analogous peptic fragments in high signal-to-noise ratio. However, the number of analogous peptide pairs is usually limited.

New proteases may provide new opportunities for better HDX-MS analysis [20–24]. A new protease may give higher sequence coverage or higher resolution than standard pepsin by itself, depending on the analyte protein and conditions. Multiple proteases can be used in parallel (in separate experiments) for the digestion of a single analyte protein [24]. Or multiple proteases can be used in tandem (in the same experiment) to generate smaller peptic fragments and higher resolution (Hamuro, unpublished results). It is not easy to find a new protease that is active in low pH and low temperature HDX-MS compatible conditions.

Gas-phase fragmentation of a peptide can yield sublocalization of deuterium within a peptide [25–30]. A new gas-phase fragmentation method has a similar value as a new protease, providing new cleavage sites for sublocalization. Electron capture dissociation (ECD) and electron transfer dissociation (ETD) showed potential for sublocalization of deuterium within a peptide. Jørgensen's group developed synthetic peptides for the detection of scrambling in gas-phase fragmentation [25] and paved the way for the practical application of this method.

Englander's group pioneered the HDX-MS analysis utilizing the isotope envelopes instead of the centroid values [13, 32]. This approach became possible because of recent development of higher resolution mass spectrometers that can give baseline resolution among the isotopic peaks. This approach, for example, can differentiate a peptide with two 50% deuterated amides versus the same peptide with one 100% deuterated amide. Old standard data analysis cannot distinguish the two situations, because it only measures the centroid value

of the peptide. This approach yields a set of deuteration levels instead of the sum of deuterium incorporation for each peptic fragment.

Monitoring a wide time range in HDX-MS analysis is often overlooked [12]. A typical protein backbone amide hydrogen exchanges between 10^{-2} s and approximately 10^{10} s [33], covering 12 orders of magnitude. On the other hand, HDX-MS data set usually measures from tens of seconds to thousands of seconds, covering approximately 2–3 orders of magnitude out of 12 orders and missing all fast exchanging and slow exchanging phenomena.

Incomplete coverage of time window is a big issue, particularly in binding site identification for protein–small molecule and protein–protein interaction. Figure 1 shows four types of HDX-MS deuterium buildup curves with no perturbation in the presence and absence of ligand. These cases except Figure 1a are considered false negative in ligand binding site identification. While the last three segments are considered nonperturbed segments, they have unobserved perturbations outside of the monitored time window (in the gray time range). The only way to prevent this issue is to monitor a wide enough time range that can cover the deuteration levels from 0% to 100% as in Figure 1a for all segments of the analyte protein.

In this paper, a new strategy to analyze HDX-MS data is described, utilizing a wider time window and isotope envelope of each analyte peptide. This study covered the time equivalent from 10^{-2} to 10^6 s at pH 7 at 23 °C. Combination with isotope

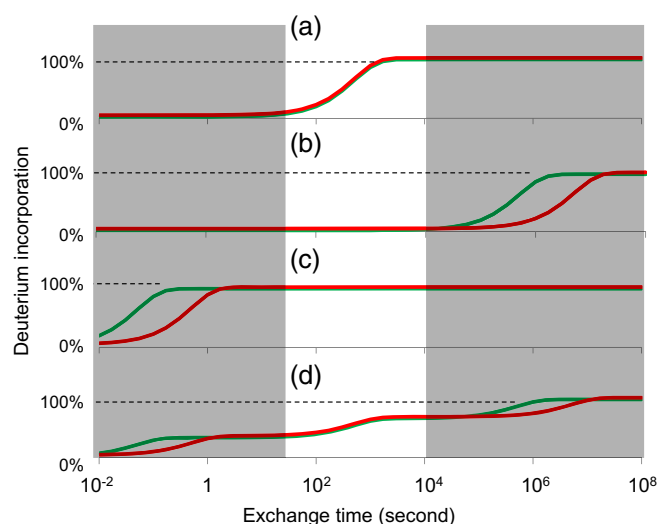


Figure 1. Simulated HDX-MS deuterium buildup curves that show no perturbations with ligand (red) and without ligand (green) in a typical HDX-MS analysis. White is the time window monitored (30 s–10,000 s) and gray is the time window not monitored. (a) Deuteration levels go up from 0% to 100% with and without ligand in the time window monitored. (b) No deuterium incorporation is observed with and without ligand in the time window monitored. (c) The peptic segment is completely deuterated with and without ligand in the time window monitored. (d) Deuterium incorporations go up in the time window monitored, whereas the deuteration levels do not cover from 0% to 100%

$$k_{ch} = k_H[H^+] + k_{OH}[OH^-] + k_{H_2O} \quad (1)$$

Hydrogen exchange reaction primarily goes through the base-catalyzed reaction near or above physiological pH (>pH 5), while the acid and water-catalyzed reactions may contribute at a very low pH. The acid- and base-catalyzed reaction rates become comparable at around pH 2.3, where hydrogen exchange reaction is the slowest [37]. Because the hydrogen exchange rate, k_{ch} , is practically proportional to the concentration of hydroxide ion, $[OH^-]$, above pH 5, hydrogen exchange reaction becomes 10 times faster as pH increases one unit in the pH range. Therefore, for example, the exchange reaction for 300 s at pH 6 is equivalent to that for 30 s at pH 7.

Effects of Temperature on Backbone Amide Hydrogen Exchange

Arrhenius equation can describe the effects of temperature on a rate constant,

$$k = A \exp(-E_a/RT) \quad (2)$$

where A is the frequency factor and E_a is the activation energy of the reaction. Now hydrogen exchange reaction is predominantly the base-catalyzed reaction above pH 5,

$$k_{ch} \sim k_{OH}[OH^-] = A \exp(-E_b/RT)[OH^-] \quad (3)$$

where E_b is the activation energy of base-catalyzed amide hydrogen exchange reaction. The activation energy of base-catalyzed amide hydrogen exchange reaction is determined to be 17 kcal/mol [35]. Equation 3 can convert the intrinsic exchange rates at various pH and temperatures to that at a standard condition.

Standardizing Exchange Time

In the current study, all exchange times were converted to the exchange times in the standard condition (pD_{corr} 7.4, 23 °C) using Equation 3. The exchange time at various pD_{corr} was converted to the exchange time at pD_{corr} 7.4 by multiplying with $10^{pD-7.4}$. All exchange times at 0 °C were converted to the exchange times at 23 °C by multiplying with 0.088 (Table 1) [12]. For example, 50 s exchange at pD_{corr} 6.4 at 0 °C is equivalent to 0.44 ($=50 \times 10^{-1} \times 0.088$) s in the standard condition.

Analysis

Checking Data Consistency

The difference in deuteration levels of a peptide in exchange conditions A and B was calculated as

$$\Delta DL(\%) = |D_A - D_B| / D_{\max} \times 100$$

where ΔDL (%) is the difference in deuteration levels, D_A is deuterium incorporation of the peptide in condition A, D_B is

deuterium incorporation of the peptide in condition B, and D_{\max} is the deuterium incorporation in the peptide in fully deuterated sample.

Determination of Exchange Rates and Maximum Deuteration Levels

Algorithm to determine a set of exchange rates ($K_{i,j}$) and a set of maximum deuteration levels ($M_{i,j}$) for residues $i-j$ is described in the following sections and Figure 2.

Observed Non-deuterated Isotope Envelope

The area of each isotopic peak was integrated. This step yielded the ratio of no ^{13}C peak, one ^{13}C peak, two ^{13}C peaks, and so forth (Figure 3a).

$$N_{i-j} = \{n_{i-j,0}, n_{i-j,1}, n_{i-j,2}, \dots\}$$

$$\sum_{k=0} n_{i-j,k} = 1$$

where N_{i-j} is the observed isotope envelope of residues $i-j$, and $n_{i-j,k}$ is the fraction of the peak with k ^{13}C atoms in the isotope envelope of non-deuterated residues $i-j$.

Variables for Simulation

Residues $i-j$ has a set of exchange rates ($K_{i,j}$) and a set of maximum deuteration levels ($M_{i,j}$) (Figure 3b),

$$K_{i-j} = \{k_i, k_{i+1}, k_{i+2}, \dots, k_j\}$$

$$M_{i-j} = \{m_i, m_{i+1}, m_{i+2}, \dots, m_j\}$$

$$\sum_{k=1}^j m_k = M_{i-j, \max}$$

where k_k is the exchange rate and m_k is the maximum deuteration level of residue k . The sum of m_k has to match the deuteration level of fully deuterated run of residues $i-j$, $M_{i-j, \max}$.

Calculation of Deuterium Distribution

The deuteration level (p) of residue i at exchange time t is

$$p_{i,t} = m_i [1 - \exp(-k_i t)]$$

$$P_{i-j,t} = \{p_{i,t}, p_{i+1,t}, p_{i+2,t}, \dots, p_{j,t}\}$$

$P_{i-j,t}$ can provide the calculated deuterium distribution in residues $i-j$ at time t , $Q_{i-j,t}$, yielding the fraction of the peak with no deuterium atoms ($q_{i-j,t,0}$), with one deuterium atom ($q_{i-j,t,1}$), and so forth (Figure 3c, d).

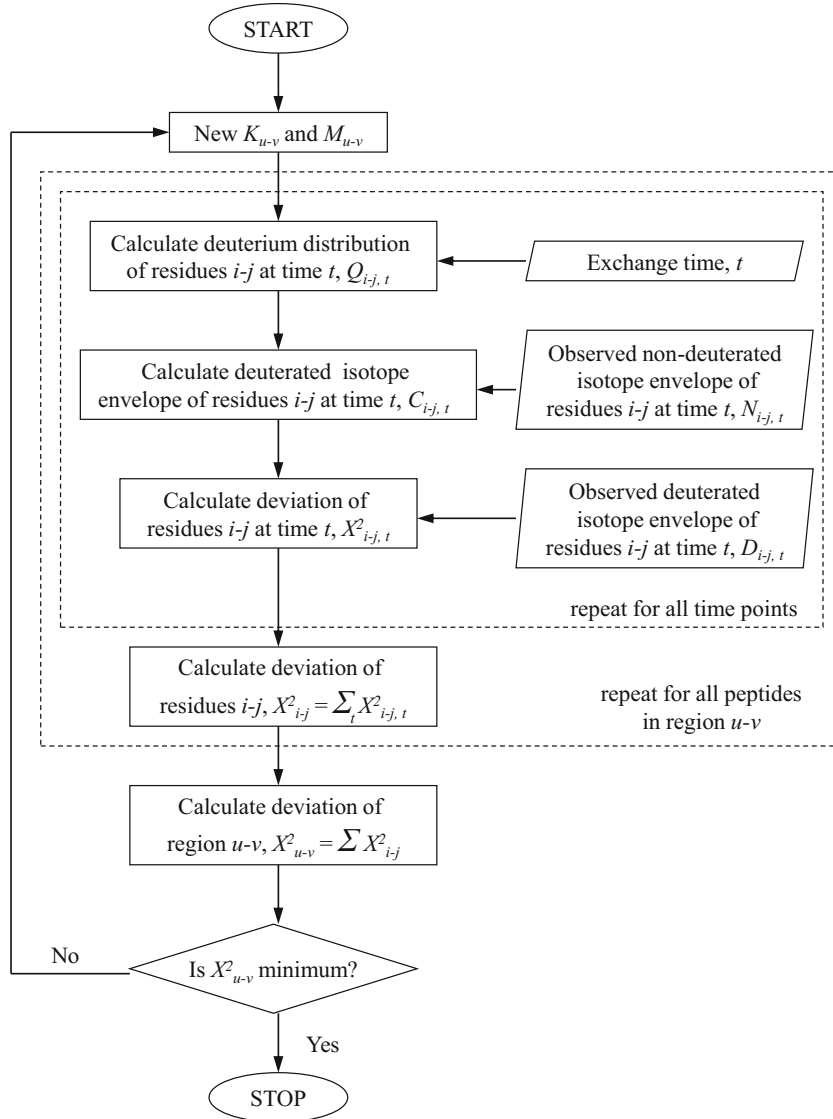


Figure 2. Flow chart of the analysis. Algorithm to determine a set of exchange rates (K_{u-v}) and a set of maximum deuteration levels (M_{u-v}) for region $u-v$. Residues $i-j$ is a part of region $u-v$

$$\begin{aligned}
 q_{i-j,t,0} &= \prod_{k=i}^j (1-p_{k,t}) \\
 q_{i-j,t,1} &= \sum_{k=i}^j \left[\frac{p_{k,t}}{(1-p_{k,t})} \prod_{k=i}^j (1-p_{k,t}) \right] \\
 \dots & \\
 Q_{i-j,t} &= \{q_{i-j,t,0}, q_{i-j,t,1}, q_{i-j,t,2}, \dots\} \\
 \sum_{k=0} q_{i-j,t,k} &= 1
 \end{aligned} \tag{4}$$

$$\begin{aligned}
 D_{i-j,t} &= \{d_{i-j,t,0}, d_{i-j,t,1}, d_{i-j,t,2}, \dots\} \\
 \sum_{k=0} d_{i-j,t,k} &= 1
 \end{aligned}$$

where $D_{i-j,t}$ is the observed isotope envelope of residues $i-j$ at time t and $d_{i-j,t,k}$ is the fraction of the $M+k$ peak in the isotope envelope of residues $i-j$ at exchange time t .

Calculation of Deuterated Isotope Envelope

Calculation with the observed nondeuterated isotope envelope, N_{i-j} , and the calculated deuterium distribution, $Q_{i-j,t}$, can provide the calculated isotope envelope of deuterated residues $i-j$ at exchange time t , $C_{i-j,t}$ (white columns in Figure 3e, f).

Observed Deuterated Isotope Envelope

The area of each deuterated isotopic peak was integrated. This step yielded the ratio of monoisotopic (M) peak, $M+1$ peak, $M+2$ peak, and so forth (black columns in Figure 3e, f).

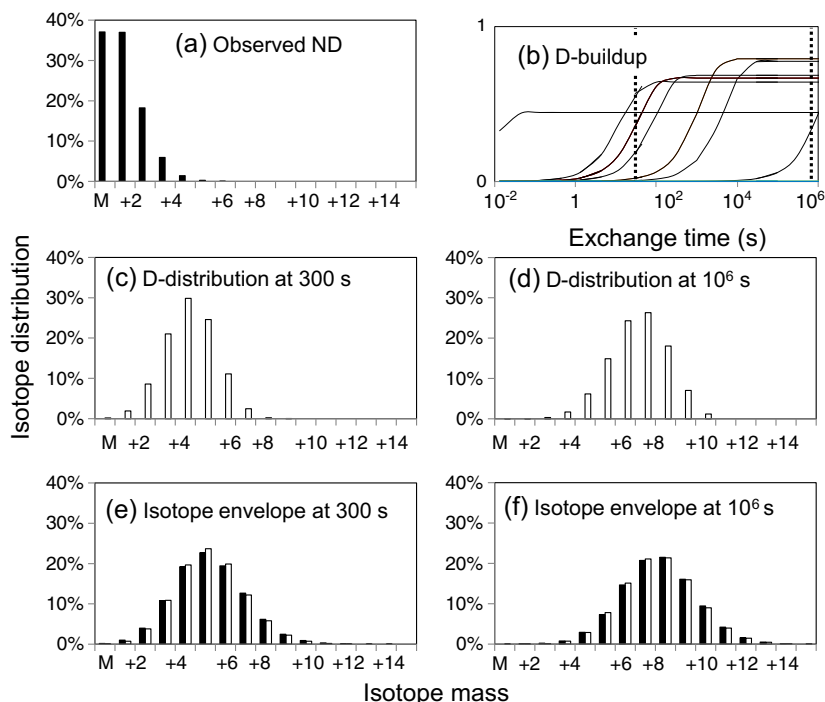


Figure 3. Simulation of deuterated isotope envelopes of residues 69–80 (corresponding to peptide 67–80). **(a)** Observed non-deuterated isotope envelope, N_{69-80} . **(b)** Deuterium buildup curves of amide hydrogens between 69 and 80 generated from K_{69-80} and M_{69-80} . There are 10 amide hydrogens in the segment because there are two prolines. Two dotted lines are at exchange times of 300 s and 1,000,000 s. **(c)** Calculated deuterium distribution at exchange time 300 s, $Q_{69-80, 300}$. **(d)** Calculated deuterium distribution at exchange time 1,000,000 s, $Q_{69-80, 1,000,000}$. **(e)** Observed (black) and calculated (white) isotope envelope at exchange time 300 s, $D_{69-80, 300}$ and $C_{69-80, 300}$. **(f)** Observed (black) and calculated (white) isotope envelope at exchange time 1,000,000 s, $D_{69-80, 1,000,000}$ and $C_{69-80, 1,000,000}$

$$\begin{aligned}
 c_{i-j,t,0} &= n_{i-j,0}q_{i-j,t,0} \\
 c_{i-j,t,1} &= n_{i-j,0}q_{i-j,t,1} + n_{i-j,1}q_{i-j,t,0} \\
 c_{i-j,t,2} &= n_{i-j,0}q_{i-j,t,2} + n_{i-j,1}q_{i-j,t,1} + n_{i-j,2}q_{i-j,t,0} \\
 &\dots \\
 C_{i-j,t} &= \{c_{i-j,t,0}, c_{i-j,t,1}, c_{i-j,t,2}, \dots\} \\
 \sum_{k=0} c_{i-j,t,k} &= 1
 \end{aligned}$$

where $c_{i-j, t, k}$ is the fraction of the $M + k$ peak in the isotope envelope of residues $i-j$ at exchange time t .

Optimization of Variables

The comparison of observed isotope envelope ($D_{i-j, t}$) and calculated isotope envelope ($C_{i-j, t}$) can tell the goodness of the parameters K_{i-j} and M_{i-j} at exchange time t , $X^2_{i-j, t}$. Minimization of the sum of the squares of deviations between the observed and calculated isotope envelopes at all time points, X^2_{i-j} , can yield the optimal K_{i-j} and M_{i-j} (Figure 2).

$$\begin{aligned}
 X^2_{i-j,t} &= \sum_k (d_{i-j,t,k} - c_{i-j,t,k})^2 \\
 X^2_{i-j} &= \sum_t X^2_{i-j,t}
 \end{aligned}$$

Multiple Peptides in the Same Region

When multiple peptides cover the same region, one set of K and M were optimized to minimize the sum of these X^2 's (Table 2). In the case of region IV in Figure 4, one set of variables, K_{67-82} and M_{67-82} , were optimized to minimize the sum of X^2 's for segments 67–80, 67–82, 68–80, 68–82, 69–80, and 69–82 (note that peptide 65–82 gives the HDX behaviors of residues 67–82; Table 2; Figure 5).

Computation

All MS raw data were imported into Excel. After each isotopic peak was integrated and converted into an area size, all data handling and calculations were performed in Excel. Variables were optimized using Solver Add-in program in Excel.

Results

The change of cytochrome *c* dynamic properties was negligible in the wide range of exchange conditions employed. The current study expands the exchange time window utilizing the effects of pH and temperature on intrinsic hydrogen exchange reactions (Theory section) [12]. The effects of pH on the dynamic properties of cytochrome *c* can be evaluated by the comparison of the deuteration levels of a peptide after two

Table 2. Backbone Amide Hydrogen Exchange Rates (s^{-1}) of Equine Cytochrome *c* at 23 °C and pD_{corr} 7.4 (K_i) and Maximum Deuteration Levels (M_i). The maximum M_i is 0.90

(I)	K_i	M_i	(II)	K_i	M_i	(III)	K_i	M_i	(V)	K_i	M_i
Gly1	2.6E+00	0.36	Lys22	n/d	n/d	Tyr48	n/d	n/d	Ala83	9.4E+02	0.59
Asp2	1.3E-01	0.69	Gly23	n/d	n/d	Thr49	8.8E-03	0.90	Gly84	2.2E-01	0.42
Val3	8.4E-02	0.64	Gly24	9.9E+02	0.32	Asp50	1.5E+02	0.59	Ile85	1.4E-03	0.70
Glu4	7.3E-02	0.63	Lys25	3.8E-02	0.29	Ala51	1.7E+01	0.62	Lys86	1.2E+02	0.67
Lys5	2.1E-02	0.55	His26	1.4E-04	0.56	Asn52	1.2E-02	0.64	Lys87	1.2E+02	0.67
Gly6	6.6E-07	0.68	Lys27	2.4E-07	0.86	Lys53	2.0E-02	0.64	Lys88	4.6E+00	0.65
Lys7	4.2E-04	0.71	Thr28	6.9E-07	0.48	Asn53	2.8E-02	0.64	Thr89	7.9E-01	0.64
Lys8	2.2E-03	0.54	Gly29	1.3E-04	0.57	Lys55	1.3E+00	0.66	Glu90	1.7E-02	0.68
Ile9	4.4E-05	0.84	Pro30	n/a	n/a	Gly56	1.3E+00	0.66	Arg91	2.8E-05	0.67
Phe10	<9.9E-09	0.35	Asn31	3.8E-02	0.29	Ile57	2.1E-03	0.61	Glu92	5.9E-07	0.67
Val11	1.2E-06	0.82	Leu32	3.2E-05	0.66	Thr58	4.0E-01	0.69	Asp93	2.9E-05	0.67
Gln12	1.9E-04	0.68	His33	3.2E-05	0.66	Trp59	3.6E-04	0.69	Leu94	5.8E-07	0.67
Lys13	2.3E-05	0.91	Gly34	2.4E-07	0.87	Lys60	1.1E-04	0.85	Ile95	9.4E-09	0.61
Cys14	2.3E-05	0.91	Leu35	1.3E-03	0.40	Glu61	9.5E-02	0.64	Ala95	5.3E-08	0.61
Ala14	1.4E-03	0.49	Phe36	1.3E-03	0.40	Glu62	3.2E-02	0.64	(VI)	K_i	M_i
Gln15	1.6E+00	0.56	Gly37	1.3E-03	0.40	Thr63	<9.9E-09	0.90	Tyr97	1.1E-07	0.89
Cys17	3.3E-01	0.58	Arg38	1.3E-03	0.40	Leu64	3.6E-05	0.33	Leu98	9.5E-08	0.90
His18	1.9E-04	0.68	Lys39	4.7E-07	0.83	Met65	1.7E-05	0.55	Lys99	<9.9E-09	0.90
Thr19	1.9E-04	0.68	Thr40	3.7E-03	0.82	Glu66	1.6E-04	0.80	Lys100	4.9E-04	0.88
Val20	1.2E+01	0.46	Gly41	1.3E-02	0.75	(IV)	K_i	M_i	Ala101	2.2E-03	0.70
Glu21	6.2E+01	0.43	Gln42	1.3E-02	0.75	Tyr67	2.3E-05	0.90	Thr102	8.7E-05	0.90
			Ala43	1.3E-02	0.75	Leu68	3.5E-06	0.61	Asn103	2.2E-02	0.72
			Pro44	n/a	n/a	Glu69	6.6E-07	0.89	Glu104	3.5E-01	0.41
			Gly45	7.2E-02	0.69	Asn70	8.0E-04	0.79			
			Phe46	1.1E+02	0.60	Pro71	n/a	n/a			
			Thr47	1.5E+02	0.90	Lys72	2.5E-02	0.67			
						Lys73	9.8E-03	0.68			
						Tyr74	8.0E-04	0.79			
						Ile75	1.9E-04	0.77			
						Pro76	n/a	n/a			
						Gly77	7.2E-02	0.64			
						Thr78	1.0E+02	0.44			
						Lys79	2.5E-02	0.67			
						Met80	2.5E-02	0.67			
						Ile81	2.2E-01	0.90			
						Phe82	3.1E+01	0.90			

different HDX-MS experiments with equivalent exchange times (Analysis section). There are 16 pairs of experimental conditions which are in different pH yet should give

identical deuteration levels (e.g., 150 s exchange at pD_{corr} 5.4 and 15 s exchange at pD_{corr} 6.4 in Table 1). The average difference in deuteration levels determined in 382

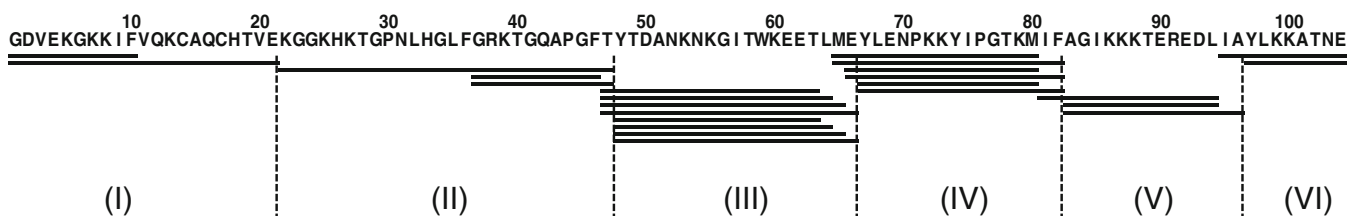


Figure 4. Sequence coverage of equine cytochrome *c* by peptic fragments. The exchange rates (K_i) and maximum deuteration levels (M_i) were optimized using the data from all peptides within each of (I) – (VI) regions

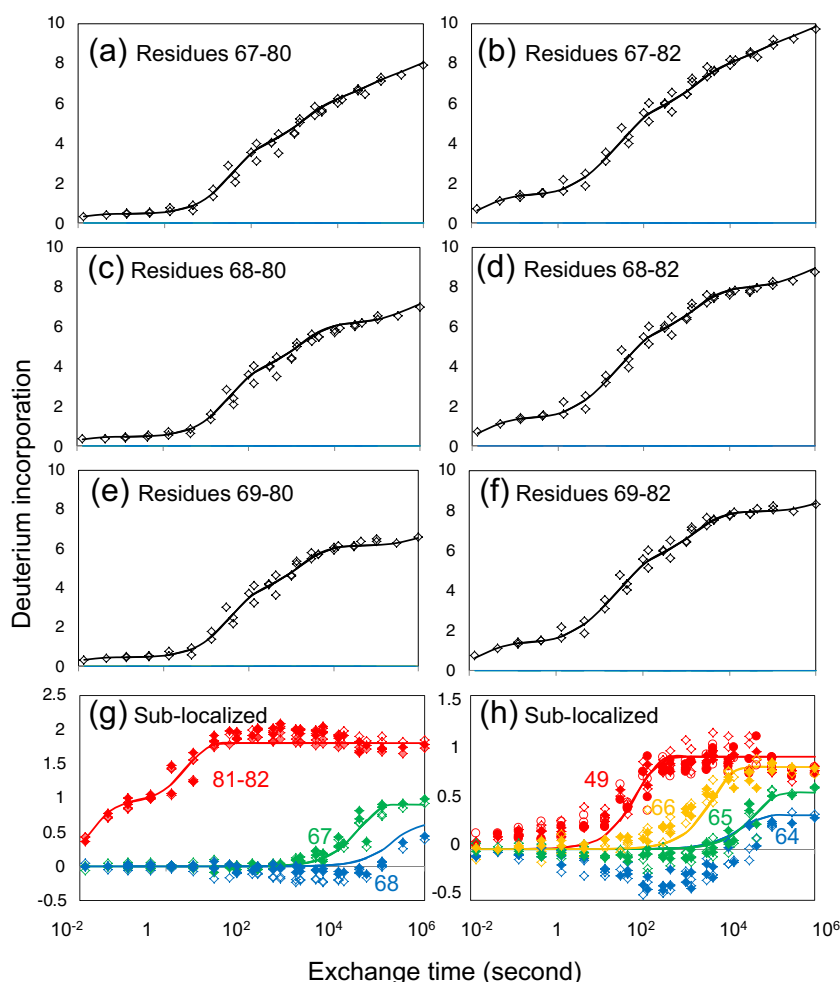


Figure 5. Representative deuterium buildup curves. Diamonds and circles are observed values and solid lines are simulated curves. (a) Residues 67–80. (b) Residues 67–82. (c) Residues 68–80. (d) Residues 68–82. (e) Residues 69–80. (f) Residues 69–82. (g) Sublocalized deuterium buildup curves. Red, residues 81–82; \diamond , (69–82) – (69–80); \blacklozenge , (68–82) – (68–80); \blacklozenge , (67–82) – (67–80). Green, residue 67; \diamond , (67–80) – (68–80); \blacklozenge , (67–82) – (68–82). Blue, residue 68; \diamond , (68–80) – (69–80); \blacklozenge , (68–82) – (69–82). (h) Sublocalized deuterium buildup curves. Red, residue 49; \diamond , (49–63) – (50–63); \blacklozenge , (49–64) – (50–64); \circ , (49–65) – (50–65); \bullet , (49–66) – (50–66). Yellow, residue 66; \diamond , (47–66) – (47–65); \blacklozenge , (48–66) – (48–65). Green, residue 65; \diamond , (47–65) – (47–64); \blacklozenge , (48–65) – (48–64). Blue, residue 64; \diamond , (47–64) – (47–63); \blacklozenge , (48–64) – (48–63).

pairs (16 pairs of experimental conditions \times 24 peptides) was 3.1% (Supplementary Table S1 in Supporting Information). Analogous analysis can be done for the temperature effects by comparing the deuteration level of 500 s at 0 °C and that of 30 s at 23 °C for pD_{corr} 7.4–10.4. In this case, each pair should give slightly different deuteration levels (see Table 1 for corrected times). The average difference in deuteration levels determined in 96 pairs (4 pairs of experimental conditions \times 24 peptides) was 4.8% (Supplementary Table S2 in Supporting Information). While these differences are slightly higher than the errors expected for duplicated experiments, the differences are not large enough to suggest significant change in the dynamic properties of cytochrome *c* by pH or temperature change (see Supplementary Figure S32 in Supporting Information for examples of HDX-MS data with significant change in dynamic properties).

In this study, equine cytochrome *c* sequence was dissected into six regions (Figure 4). One set of parameters (exchange rates, K_i and maximum deuteration levels, M_i) was used to fit the isotope envelopes of all peptides in each region at all time points as described in the Analysis section. For example, one set of 28 variables, K_{67-82} and M_{67-82} (Table 2), fit all isotope envelopes of six peptides, 65–80, 65–82, 66–80, 66–82, 67–80, and 67–82 in region IV (Figure 4) at all 40 time points. While K_{67-82} and M_{67-82} were optimized to fit the isotope envelopes, the variables can describe the deuterium buildup curves of the peptides very well (Figure 5a–f).

The overlapping peptides further dissected cytochrome *c* sequence into 19 segments (Table 2) using 24 high-quality peptides (Figure 4 and Supplementary Figures S1–S31 in Supporting Information). For example, the six peptides shown in Figure 5 dissected region IV into four segments, 67, 68, 69–80, and 81–82 (Table 2). Out of 19 segments, seven segments

(Thr47, Thr49, Leu64, Met65, Glu66, Tyr67, and Leu68) were single amide resolution and gave the explicit exchange rate at each position. There are four segments (81–82, 83–84, 95–96, and 97–98) that are only two residues long. In these cases, each exchange rate was assigned to be as consistent as possible with the previous NMR data [33]. There are eight relatively large segments, such as 1–10. It is not possible to assign each exchange rate explicitly without external information in these segments. For these segments, first each exchange rate was assigned to be consistent with the NMR data. Then, the rest was assigned so that neighboring residues have similar exchange rates.

This approach determined 97 backbone amide hydrogen exchange rates out of 100 amino acids (excluding four prolines; Table 2). There are three residues (Lys22, Gly23, and Tyr48) not monitored because the first two residues of each peptide lose deuterium too fast to follow during the downstream processing [35]. For example, “peptide” 22–47 provides the HDX behaviors of amide hydrogens in “segment” 24–47. The only exceptions are peptides starting at *N*-terminal of cytochrome *c*, which is acetylated.

Calculated parameters can describe the deuteration levels of sublocalized residues very well. For example, the deuterium buildup curves calculated from the parameters, k_{67} , k_{68} , k_{81} , k_{82} , m_{67} , m_{68} , m_{81} , and m_{82} , fit the observed deuteration levels of residues 67, 68, and 81–82 very well (Figure 5g). These eight parameters were determined by fitting the isotope envelopes of six peptides in region IV (Figure 4), not by fitting the deuterium buildup curve of each sub-localized residue. Similarly, the parameters, k_{49} , k_{64} , k_{65} , k_{66} , m_{49} , m_{64} , m_{65} , and m_{66} , determined by fitting the isotope envelopes of eight peptides in region III (Figure 4) can describe the observed deuteration levels of residues 49, 64, 65, and 66 very well (Figure 5h). The good agreement between simulated and observed

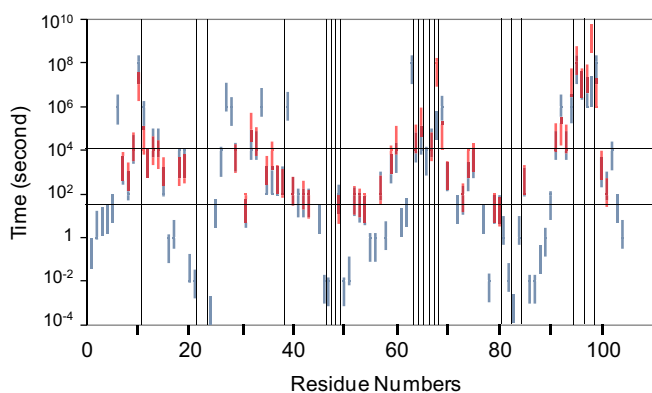


Figure 6. Backbone amide hydrogen exchange behaviors of equine cytochrome *c*. A blue bar is 10%–90% deuteration of each residue at 23 °C, pD_{corr} 7.4 determined by HDX-MS. A red bar is that at the same conditions calculated from the NMR data [33]. Note that the NMR data were acquired at 20 °C, pD_{corr} 7.0, and the figure was made after all exchange rates were converted to those at 23 °C, pD_{corr} 7.4. Vertical lines separate the segments described in the main text. Horizontal lines are at 30 s and 10,000 s. A typical HDX-MS experiment monitors the HDX behaviors of an analyte protein between these two times

deuterium buildup curves in sublocalized segments supports the integrity of this approach.

A typical HDX-MS protocol can monitor only one-third (34/97) of backbone amide hydrogens despite 100% sequence coverage for equine cytochrome *c*. A typical HDX-MS protocol surveys 2–3 orders of time window (e.g., 30 to 10,000 s shown in Figure 6). In this protocol, 36 out of 97 backbone amide hydrogens exchange too fast to follow, and 27 hydrogens exchange too slowly, leaving approximately two-thirds of amide hydrogen behaviors unobserved.

The NMR method determined about one-half (53/100) of backbone exchange rates for equine cytochrome *c* [33]. The technique can explicitly determine the exchange rates of slowly exchanging amide hydrogens, while it cannot observe any fast exchanging amide hydrogens (Figure 5). Acquiring NMR data at pD 5 in addition to pD 7 might add a dozen more exchange rates by monitoring faster exchanging amide hydrogens.

The amide hydrogen exchange rates obtained by HDX-MS method and NMR method are in good agreement (Figure 7). Only seven out of 53 residues have HDX-MS exchange rates more than one order of magnitude different from those determined by NMR. Particularly important ones are 10 residues, the exchange rates of which were determined at high resolution (either single amide residue segments or two residue segments) by HDX-MS (residues Thr49, Leu64, Met65, Glu66, Tyr67, Leu68, Ile95, Ala96, Tyr97, and Leu98; ♦ in Figure 7). While the HDX-MS experiment yielded 15 high resolution exchange rates, five of them exchanged too fast for NMR experiment.

Discussion

When a patent or regulatory filing requires describing the dynamic properties of a biopharmaceutical, a set of backbone amide hydrogen exchange rates is more appropriate than a set of peptide deuteration levels. The majority of current HDX-MS studies reports a set of peptide deuteration levels, such as

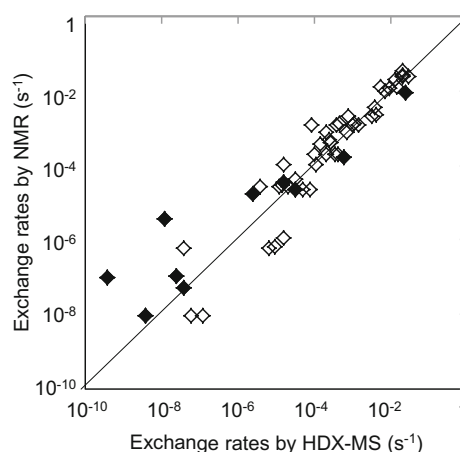


Figure 7. Comparison of backbone amide hydrogen exchange rates determined by HDX-MS and NMR at 23 °C, pD_{corr} 7.4; ♦, the residue determined at high resolution by HDX-MS; ◇, the residue located in a relatively large segment

deuterium buildup curves [2], color maps [19], or butterfly charts [38]. Although these presentations are very useful to quickly grasp the similarities and differences in the dynamic properties of an analyte protein, they do not have solid physicochemical meanings. The values could change depending on experimental conditions, such as back exchange during downstream process [37, 39]. Therefore, the comparison of two data from different instruments or laboratories is difficult. On the other hand, once the data is reduced down to a set of exchange rates (K_i), they should not change as long as the protein fold and exchange conditions are the same (although maximum deuteration levels (M_i) may vary depending on laboratories or instruments). An HDX-MS practitioner may choose the data analysis method depending on the purpose of the analysis.

It is important to monitor a wide time window in HDX-MS experiment, particularly for ligand binding site identification. While the HDX-MS technique is gaining in popularity for the identification of protein–protein and protein–small molecule interaction sites especially for epitope mapping of antibody drugs, the inability to detect perturbation upon interaction may be a big problem. In the case of well-studied equine cytochrome *c* – E8 antibody interaction, a standard HDX-MS protocol can monitor only about one-third (5/14) of exchange rates in the antibody binding site. X-ray co-crystal structure of cytochrome *c* – E8 antibody complex identified 14 residues (Val3, Gly34, Phe36, Gly37, Lys39, Thr58, Lys60, Glu61, Glu62, Ala96, Lys99, Lys100, Asn103, and Glu104) as the contact residues [40]. Among the 14 residues, only five residues (Phe36, Gly37, Thr58, Lys60, and Lys100) exchange between 30 and 10,000 s. On the other hand, the current method can cover all residues except Lys99.

The deconvolution of isotope envelope can provide a lot more information than the centroid value of the same isotope envelope [13]. In an ideal situation, the deconvolution of peptide isotope envelope with x potentially deuterated amides can give x number of deuteration values. On the other hand, the centroid of the same isotope envelope can provide only one value, the sum of the all deuteration levels. This means that obtaining only centroid values in HDX-MS analysis wastes a lot of valuable information. When HDX-MS started in the 1990s, most practitioners were using low resolution mass spectrometers that cannot clearly separate each peak (therefore deconvolute) in an isotope envelope. Combined with not ideal signal-to-noise ratio, usage of centroid values for HDX-MS analysis became the standard. Now, with recent development of MS, higher resolution HDX-MS data have become commonly available for HDX-MS studies, and the deconvolution of isotope envelope is much easier.

While the current analysis is similar to a pioneering HDsite work [13] by Englander's group, there are three major differences between HDsite analysis and the current analysis. The first one is usage of a wider time window, which is critical to obtain not single amide deuteration levels but single amide exchange rates because the exchange rates may vary by 12 orders of magnitude (Figure 6). To expand the time window, HDX-MS experiments can be also performed at (1) very short

time points by a stopped-flow type apparatus, (2) very long time points, (3) various temperatures, and (4) various pHs [12]. Each of the conditions (2)–(4) requires the analyte protein to have the same dynamic properties as the native state in the given exchange condition. A wider time window was possible in the current study primarily because of the stability of cytochrome *c* in the wide pH range.

The second difference is the usage of one maximum deuteration level for each amide hydrogen in all peptides involved, instead of calculating the back exchange for each amide hydrogen in each peptide (see Multiple Peptides in the Same Region in Analysis; Figure 2). For example, the maximum deuteration level of Glu69, m_{69} , is assumed constant in six peptides, 65–80, 65–82, 66–80, 66–82, 67–80, and 67–82, although the peptides have different retention times that may lead to different the maximum deuteration levels for Glu69 in these peptides. HDsite analysis calculates the effective back exchange time for each peptide and thus uses different maximum deuteration levels for the same amide hydrogen in different peptides. The simplification of back exchange treatment in the current study is possible because the back exchange is significantly slowed down once organic solvent is introduced in the liquid chromatography step. The current simpler method is probably practical for an HDX-MS system with well-controlled temperature, as the deuterium loss from a peptide is negligible in the liquid chromatography step.

The third difference is a one-step, global-fitting algorithm to obtain amide hydrogen exchange rates in the current analysis. HDsite analysis yields the amide hydrogen exchange rates in two steps: (1) calculating the deuteration level (or D-occupancy) of each amide hydrogen at each time point by fitting the isotope envelopes of peptides, which include the amide hydrogen, and (2) calculating the exchange rate of the amide hydrogen by fitting the deuteration level change of the amide hydrogen in the time course. The current study obtains a set of amide hydrogen exchange rates along with a set of maximum deuteration levels in one step. The current study performs a global-fit of all isotope envelopes at all time points in all peptides in one region using a set of amide hydrogen exchange rates and a set of maximum deuteration levels (see Analysis section; Figure 2). This simple one-step, global-fitting approach is possible because of the usage of one maximum deuteration level for each amide hydrogen in all peptides involved, as described in the second difference.

The current analysis has pros and cons over HDsite analysis. A big advantage of the current analysis is that there is no need to assign each deuteration level to each residue to calculate the exchange rate. For example, in the current data, there are 10 deuteration levels for segment 69–80 at each time point (Table 2). To obtain an exchange rate in HDsite, one out of 10 deuteration levels from each time point has to be picked correctly to generate one deuterium buildup curve. This selection may not be trivial, especially with erroneous data and/or data with large segments. An HDsite type two-step approach was not applicable to the current study because of the large size of some regions. The current analysis does not have this ambiguity and yields a set of exchange rates even for a large region.

A potential issue of the current analysis is the assumption that each amide hydrogen (e.g., Glu69) has the one maximum deuteration level (the same back exchange) in all peptides involved (in this case, peptides 65–80, 65–82, 66–80, 66–82, 67–80, and 67–82). This may be a problem in a system with poorly controlled temperature or an analysis with a long chromatography time. However, this appears not to be a problem in the current study, judging from the sublocalized results (Figure 5g, h). Overall, the current analysis algorithm is simpler and easier to implement than the HDsite algorithm to obtain hydrogen exchange rates, as long as the one maximum deuteration level assumption holds for the data analyzed.

Future works may combine a wider time window with high resolution HDX-MS studies using gas-phase fragmentation to present explicit exchange rates. Gas-phase fragmentation aiming to use for HDX-MS is an active research area [25–30]. While more papers demonstrate the use of gas-phase fragmentation for high resolution HDX-MS data, all of them are determining not the exchange rates of residues but the deuteration levels of residues [6, 7]. From a practical point of view, gas-phase fragmentation technique is the same as a new protease, which enables new sublocalizations. A paper determining the explicit exchange rates using gas-phase fragmentation is awaited to fully realize and validate the power of gas-phase fragmentation for HDX-MS.

Conclusion

Almost a quarter century has passed since the first HDX-MS paper was published [1]. Since then, HDX-MS has gained utility and popularity and now is a very important tool to study proteins. MS and automation technology has improved significantly during the period and can provide much superior raw data for HDX-MS analysis [3, 41, 42]. While the software to extract information from HDX-MS raw data has improved and the presentation of the data has become refined, the majority of the data extracted is still centroid values and most of the data presented is still deuteration levels of peptides [14–17]. While this data analysis approach is fine and valuable to quickly investigate biological function of a target protein, this may not be suitable for a more precise protein characterization purpose, such as a patent or regulatory filing. With the availability of high resolution HDX-MS raw data, it may be the time to shift the data analysis paradigm from determination of centroid values and presentation of deuteration levels to deconvolution of isotope envelopes and presentation of exchange rates.

Acknowledgements

The author thanks Stephen J. Coales, Sook Yen E, Jessica E. Lee, and Anita Ma for their technical support.

References

- Zhang, Z., Smith, D.L.: Determination of amide hydrogen exchange by mass spectrometry: a new tool for protein structure elucidation. *Protein Sci.* **2**, 522–531 (1993)
- Engen, J.R., Smith, D.L.: Investigating protein structure and dynamics by hydrogen exchange MS. *Anal. Chem.* **73**, 256A–265A (2001)
- Hamuro, Y., Coales, S.J., Southern, M.R., Nemeth-Cawley, J.F., Stranz, D.D., Griffin, P.R.: Rapid analysis of protein structure and dynamics by hydrogen/deuterium exchange mass spectrometry. *J. Biomol. Tech.* **14**, 171–182 (2003)
- Englander, S.W., Mayne, L., Kan, Z.Y., Hu, W.: Protein folding-how and why: by hydrogen exchange, fragment separation, and mass spectrometry. *Annu. Rev. Biophys.* **45**, 135–152 (2016)
- Hamuro, Y., Coales, S.J., Morrow, J.A., Molnar, K.S., Tuske, S.J., Southern, M.R., Griffin, P.R.: Hydrogen/deuterium-exchange (H/D-Ex) of PPAR LBD in the presence of various modulators. *Protein Sci.* **15**, 1 (2006)
- Landgraf, R.R., Chalmers, M.J., Griffin, P.R.: Automated hydrogen/deuterium exchange electron transfer dissociation high resolution mass spectrometry measured at single-amide resolution. *J. Am. Soc. Mass Spectrom.* **23**, 301–309 (2012)
- Huang, R.Y., Garai, K., Frieden, C., Gross, M.L.: Hydrogen/deuterium exchange and electron-transfer dissociation mass spectrometry determine the interface and dynamics of apolipoprotein E oligomerization. *Biochemistry* **50**, 9273–9282 (2011)
- Burns-Hamuro, L., Hamuro, Y., Kim, J., Sigala, P., Fayos, R., Stranz, D., Jennings, P., Taylor, S., Woods Jr., V.L.: Distinct interaction modes of an AKAP bound to two regulatory subunit isoforms of protein kinase A revealed by amide hydrogen/deuterium exchange. *Protein Sci.* **14**, 2982–2992 (2005)
- Horn, J.R., Kraybill, B., Petro, E.J., Coales, S.J., Morrow, J.A., Hamuro, Y., Kossiakoff, A.A.: The role of protein dynamics in increasing binding affinity for an engineered protein-protein interaction established by H/D exchange mass spectrometry. *Biochemistry* **45**, 8488–8498 (2006)
- Hamuro, Y., Anand, G., Kim, J., Juliano, C., Stranz, D., Taylor, S., Woods Jr., V.L.: Mapping intersubunit interactions of the regulatory subunit (R1 α) in the type I holoenzyme of protein kinase A by amide hydrogen/deuterium exchange mass spectrometry (DXMS). *J. Mol. Biol.* **340**, 1185–1196 (2004)
- Casina, V.C., Hu, W., Mao, J.H., Lu, R.N., Hanby, H.A., Pickens, B., Kan, Z.Y., Lim, W.K., Mayne, L., Ostertag, E.M., Kacir, S., Siegel, D.L., Englander, S.W., Zheng, X.L.: High-resolution epitope mapping by HX MS reveals the pathogenic mechanism and a possible therapy for autoimmune TTP syndrome. *Proc. Natl. Acad. Sci. U. S. A.* **112**, 9620–9625 (2015)
- Coales, S.J., Sook Yen, E., Lee, J.E., Ma, A., Morrow, J.A., Hamuro, Y.: Expansion of time window for mass spectrometric measurement of amide hydrogen/deuterium exchange reactions. *Rapid Commun. Mass Spectrom.* **24**, 3585–3592 (2010)
- Kan, Z.Y., Walters, B.T., Mayne, L., Englander, S.W.: Protein hydrogen exchange at residue resolution by proteolytic fragmentation mass spectrometry analysis. *Proc. Natl. Acad. Sci. U. S. A.* **110**, 16438–16443 (2013)
- Pascal, B.D., Willis, S., Lauer, J.L., Landgraf, R.R., West, G.M., Marciano, D., Novick, S., Goswami, D., Chalmers, M.J., Griffin, P.R.: HDX workbench: software for the analysis of H/D exchange MS data. *J. Am. Soc. Mass Spectrom.* **23**, 1512–1521 (2012)
- Weis, D.D., Engen, J.R., Kass, I.J.: Semi-automated data processing of hydrogen exchange mass spectra using HX-Express. *J. Am. Soc. Mass Spectrom.* **17**, 1700–1703 (2006)
- Lindner, R., Lou, X., Reinstein, J., Shoeman, R.L., Hamprecht, F.A., Winkler, A.: Hexicon 2: automated processing of hydrogen-deuterium exchange mass spectrometry data with improved deuteration distribution estimation. *J. Am. Soc. Mass Spectrom.* **25**, 1018–1028 (2014)
- Zhang, Z., Zhang, A., Xiao, G.: Improved protein hydrogen/deuterium exchange mass spectrometry platform with fully automated data processing. *Anal. Chem.* **84**, 4942–4949 (2012)
- Anand, G.S., Hughes, C.A., Jones, J.M., Taylor, S.S., Komives, E.A.: Amide H²H exchange reveals communication between the cAMP and catalytic subunit-binding sites in the R1 α subunit of protein kinase A. *J. Mol. Biol.* **323**, 377–386 (2002)

19. Hamuro, Y., Burns, L.L., Canaves, J.M., Hoffman, R.C., Taylor, S.S., Woods Jr., V.L.: Domain organization of D-AKAP2 revealed by enhanced deuterium exchange-mass spectrometry (DXMS). *J. Mol. Biol.* **321**, 703–714 (2002)
20. Zhang, H.M., Kazazic, S., Schaub, T.M., Tipton, J.D., Emmett, M.R., Marshall, A.G.: Enhanced digestion efficiency, peptide ionization efficiency, and sequence resolution for protein hydrogen/deuterium exchange monitored by Fourier transform ion cyclotron resonance mass spectrometry. *Anal. Chem.* **80**, 9034–9041 (2008)
21. Rey, M., Yang, M., Burns, K.M., Yu, Y., Lees-Miller, S.P., Schriemer, D.C.: Nepenthesin from monkey cups for hydrogen/deuterium exchange mass spectrometry. *Mol. Cell Proteomics* **12**, 464–472 (2013)
22. Kadek, A., Mrazek, H., Halada, P., Rey, M., Schriemer, D.C., Man, P.: Aspartic protease nepenthesin-1 as a tool for digestion in hydrogen/deuterium exchange mass spectrometry. *Anal. Chem.* **86**, 4287–4294 (2014)
23. Yang, M., Hoepfner, M., Rey, M., Kadek, A., Man, P., Schriemer, D.C.: Recombinant nepenthesin II for hydrogen/deuterium exchange mass spectrometry. *Anal. Chem.* **87**, 6681–6687 (2015)
24. Mayne, L., Kan, Z.Y., Chetty, P.S., Ricciuti, A., Walters, B.T., Englander, S.W.: Many overlapping peptides for protein hydrogen exchange experiments by the fragment separation-mass spectrometry method. *J. Am. Soc. Mass Spectrom.* **22**, 1898–1905 (2011)
25. Rand, K.D., Jorgensen, T.J.: Development of a peptide probe for the occurrence of hydrogen ($^1\text{H}/^2\text{H}$) scrambling upon gas-phase fragmentation. *Anal. Chem.* **79**, 8686–8693 (2007)
26. Rand, K.D., Adams, C.M., Zubarev, R.A., Jorgensen, T.J.: Electron capture dissociation proceeds with a low degree of intramolecular migration of peptide amide hydrogens. *J. Am. Chem. Soc.* **130**, 1341–1349 (2008)
27. Rand, K.D., Zehl, M., Jensen, O.N., Jorgensen, T.J.: Loss of ammonia during electron-transfer dissociation of deuterated peptides as an inherent gauge of gas-phase hydrogen scrambling. *Anal. Chem.* **82**, 9755–9762 (2010)
28. Rand, K.D., Zehl, M., Jorgensen, T.J.: Measuring the hydrogen/deuterium exchange of proteins at high spatial resolution by mass spectrometry: overcoming gas-phase hydrogen/deuterium scrambling. *Acc. Chem. Res.* **47**, 3018–3027 (2014)
29. Seger, S.T., Breinholt, J., Faber, J.H., Andersen, M.D., Wiberg, C., Schjodt, C.B., Rand, K.D.: Probing the conformational and functional consequences of disulfide bond engineering in growth hormone by hydrogen-deuterium exchange mass spectrometry coupled to electron transfer dissociation. *Anal. Chem.* **87**, 5973–5980 (2015)
30. Rand, K.D., Pringle, S.D., Morris, M., Brown, J.M.: Site-specific analysis of gas-phase hydrogen/deuterium exchange of peptides and proteins by electron transfer dissociation. *Anal. Chem.* **84**, 1931–1940 (2012)
31. Hamuro, Y., Coales, S.J., Molnar, K.S., Tuske, S.J., Morrow, J.A.: Specificity of immobilized porcine pepsin in H/D exchange compatible conditions. *Rapid Commun. Mass Spectrom.* **22**, 1041–1046 (2008)
32. Kan, Z.Y., Mayne, L., Chetty, P.S., Englander, S.W.: ExMS: data analysis for HX-MS experiments. *J. Am. Soc. Mass Spectrom.* **22**, 1906–1915 (2011)
33. Milne, J.S., Mayne, L., Roder, H., Wand, A.J., Englander, S.W.: Determinants of protein hydrogen exchange studied in equine cytochrome *c*. *Protein Sci.* **7**, 739–745 (1998)
34. Glasoe, P.K., Long, F.A.: Use of glass electrodes to measure acidities in deuterium oxide. *J. Phys. Chem.* **64**, 188–189 (1960)
35. Bai, Y., Milne, J.S., Mayne, L.C., Englander, S.W.: Primary structure effects on peptide group hydrogen exchange. *Proteins Struct. Funct. Genet.* **17**, 7–86 (1993)
36. Englander, S.W., Kallenbach, N.R.: Hydrogen exchange and structural dynamics of proteins and nucleic acids. *Q. Rev. Biophys.* **16**, 521–655 (1984)
37. Walters, B.T., Ricciuti, A., Mayne, L., Englander, S.W.: Minimizing back exchange in the hydrogen exchange-mass spectrometry experiment. *J. Am. Soc. Mass Spectrom.* **23**, 2132–2139 (2012)
38. Wei, H., Ahn, J., Yu, Y.Q., Tymiak, A., Engen, J.R., Chen, G.: Using hydrogen/deuterium exchange mass spectrometry to study conformational changes in granulocyte colony stimulating factor upon PEGylation. *J. Am. Soc. Mass Spectrom.* **23**, 498–504 (2012)
39. Sheff, J.G., Schriemer, D.C.: Toward standardizing deuterium content reporting in hydrogen exchange-MS. *Anal. Chem.* **86**, 11962–11965 (2014)
40. Paterson, Y., Englander, S.W., Roder, H.: An antibody binding site on cytochrome *c* defined by hydrogen exchange and two-dimensional NMR. *Science (Washington, DC)* **249**, 755–759 (1990)
41. Chalmers, M.J., Busby, S.A., Pascal, B.D., He, Y., Hendrickson, C.L., Marshall, A.G., Griffin, P.R.: Probing protein ligand interactions by automated hydrogen/deuterium exchange mass spectrometry. *Anal. Chem.* **78**, 1005–1014 (2006)
42. Wales, T.E., Fadgen, K.E., Gerhardt, G.C., Engen, J.R.: High-speed and high-resolution UPLC separation at zero degrees Celsius. *Anal. Chem.* **80**, 6815–6820 (2008)